

Photoreflectance system based on vacuum ultraviolet laser at 177.3 nm

Wei-Xia Luo(罗伟霞), Xue-Lu Liu(刘雪璐), Xiang-Dong Luo(罗向东), Feng Yang(杨峰), Shen-Jin Zhang(张申金), Qin-Jun Peng(彭钦军), Zu-Yan Xu(许祖彦), and Ping-Heng Tan(谭平恒)

Citation: Chin. Phys. B, 2022, 31 (**11**): 110701. DOI: 10.1088/1674-1056/ac89e4

What follows is a list of articles you may be interested in

A 32-channel 100 GHz wavelength division multiplexer by interleaving two silicon arrayed waveguide gratings

Changjian Xie(解长健), Xihua Zou (邹喜华), Fang Zou(邹放), Lianshan Yan(闫连山), Wei Pan(潘炜), and Yong Zhang(张永)

Chin. Phys. B, 2021, 30 (**12**): 120703. DOI: 10.1088/1674-1056/ac2d23

Third-order nonlinear optical properties of graphene composites: A review

Meng Shang(尚萌), Pei-Ling Li(李培玲), Yu-Hua Wang(王玉华), and Jing-Wei Luo(罗经纬)

Chin. Phys. B, 2021, 30 (**8**): 080703. DOI: 10.1088/1674-1056/ac0424

Low temperature photoluminescence study of GaAs defect states

Jia-Yao Huang(黄佳瑶), Lin Shang(尚林), Shu-Fang Ma(马淑芳), Bin Han(韩斌), Guo-Dong Wei(尉国栋), Qing-Ming Liu(刘青明), Xiao-Dong Hao(郝晓东), Heng-Sheng Shan(单恒升), Bing-She Xu(许并社)

Chin. Phys. B, 2020, 29 (**1**): 010703. DOI: 10.1088/1674-1056/ab5fb8

Development of a 170-mm hollow corner cube retroreflector for the future lunar laser ranging

Yun He(何芸), Qi Liu(刘祺), Jing-Jing He(何静静), Ming Li(黎明), Hui-Zong Duan(段会宗), Hsien-Chi Yeh(叶贤基), Jun Luo(罗俊)

Chin. Phys. B, 2018, 27 (**10**): 100701. DOI: 10.1088/1674-1056/27/10/100701

Co-focus experiment of segmented mirror

Bin Li(李斌), Wen-Hao Yu(于文豪), Mo Chen(陈莫), Jin-Long Tang(唐金龙), Hao Xian(鲜浩)

Chin. Phys. B, 2017, 26 (**6**): 060706. DOI: 10.1088/1674-1056/26/6/060706

INSTRUMENTATION AND MEASUREMENT

Photoreflectance system based on vacuum ultraviolet laser at 177.3 nm

Wei-Xia Luo(罗伟霞)[1,2], Xue-Lu Liu(刘雪璐)[1,†], Xiang-Dong Luo(罗向东)[3], Feng Yang(杨峰)[4,5], Shen-Jin Zhang(张申金)[4,5], Qin-Jun Peng(彭钦军)[4,5], Zu-Yan Xu(许祖彦)[4,5], and Ping-Heng Tan(谭平恒)[1,2,‡]

[1] *State Key Laboratory of Superlattices and Microstructures, Institute of Semiconductors, Chinese Academy of Sciences (CAS), Beijing* 100083, *China*
[2] *Center of Materials Science and Optoelectronics Engineering & CAS Center of Excellence in Topological Quantum Computation, University of Chinese Academy of Sciences, Beijing* 100049, *China*
[3] *Jiangsu Key Laboratory of ASIC, Nantong University, Nantong* 226019, *China*
[4] *Key Laboratory of Solid State Laser, Technical Institute of Physics and Chemistry, Chinese Academy of Sciences, Beijing* 100190, *China*
[5] *Key Laboratory of Function Crystal and Laser Technology, Technical Institute of Physics and Chemistry, Chinese Academy of Sciences, Beijing* 100190, *China*

(Received 30 May 2022; revised manuscript received 29 July 2022; accepted manuscript online 16 August 2022)

Photoreflectance (PR) spectroscopy is a powerful and non-destructive experimental technique to explore interband transitions of semiconductors. In most PR systems, the photon energy of the pumping beam is usually chosen to be higher than the bandgap energy of the sample. To the best of our knowledge, the highest energy of pumping laser in reported PR systems is 5.08 eV (244 nm), not yet in the vacuum ultraviolet (VUV) region. In this work, we report the design and construction of a PR system pumped by VUV laser of 7.0 eV (177.3 nm). At the same time, dual-modulated technique is applied and a dual channel lock-in-amplifier is integrated into the system for efficient PR measurement. The system's performance is verified by the PR spectroscopy measurement of well-studied semiconductors, which testifies its ability to probe critical-point energies of the electronic band in semiconductors from ultraviolet to near-infrared spectral region.

Keywords: photoreflectance spectroscopy, vacuum ultraviolet laser, electronic band structure, critical points of electron density of states

PACS: 07.60.–j, 78.40.–q, 71.20.–b, 78.20.–e **DOI:** 10.1088/1674-1056/ac89e4

1. Introduction

Electromodulation (EM) spectroscopy, including photoreflectance (PR), electroreflectance (ER), and contactless electroreflectance (CER), has contributed significantly to the investigation of electronic structures, interband transitions, and alloy composition in semiconductors.[1,2] The derivative nature of this technique emphasizes features at the energy of critical points in band structure, which is realized by modulating the built-in electric field of sample to cause perturbation in its reflectance amplitude. Compared to applying an external electric field in ER and CER spectroscopy, PR spectroscopy utilizes photoinjection of electron–hole pairs via a chopped pumping beam, usually an incident laser, to modulate the built-in electric field. Therefore, a conventional PR system typically chooses the photon energy of the pumping laser to be higher than the bandgap of the semiconductor under investigation. Since the modulated electric field affects the overall electronic structure of the tested sample, even critical points at energy higher than the pumping beam are proven to be detectable in narrow bandgap semiconductors.[3,4] Below-bandgap pumping through impurities or defects states at sub-bandgap energies is used very rarely since the traps and recombination centers could reduce the effectiveness of modulation and PR signal amplitude varies from sample to sample.[5,6] Also the spectral feature obtained by below-bandgap pumping differs from that of the conventional PR spectra with above-bandgap pumping due to their different modulation distribution.[7,8] Therefore, for the investigation of wide bandgap materials in the UV region, vacuum ultraviolet (VUV) pumping sources in the wavelength region between 100 nm and 200 nm are more desired.

To the best of our knowledge, the highest pumping energy in reported PR systems is 5.08 eV (244 nm) from a frequency-doubled Ar^+ laser line,[9,10] not yet in the VUV region. Based on the breakthrough on the nonlinear crystal $KBe_2BO_3F_2$ (KBBF) growth and KBBF prism-coupled device (KBBF-PCD), DUV diode-pumped solid-state lasers (DUV-DPL) with emission at 7.0 eV (177.3 nm) have been developed using KBPBF-PCD with Nd:YAG as the basic light sources.[11,12] This DUV-DPL has already successfully been coupled with various scientific techniques to construct cutting-edge instruments.[13–16] With its high photon density, large photon flux and high energy resolution, this VUV laser is expected to be utilized in PR system to active the exploration of

†Corresponding author. E-mail: liuxuelu@semi.ac.cn
‡Corresponding author. E-mail: phtan@semi.ac.cn

© 2022 Chinese Physical Society and IOP Publishing Ltd

interband transition located in high-energy region. It is also worth noting that although the use of visible light as pumping and probing beams is effective for a broad range of semiconductor materials, but the penetration depth of visible light is typically hundreds of nanometers. For microscale structure, light travels through the multilayered films or superlattices and thus PR signals from different mediums inevitably overlap and be affected by interference effect.[17] While pumping with UV laser can provide not only a much stronger absorption with photon energy much above the bandgap, but also relatively shallow depth down to few nanometers,[18] which can be used to effectively distinguish surface PR signals from inner space, in ways not possible when using visible laser as the pumping beam.

In this work, we design and construct a PR system under the pumping of a VUV laser at 177.3 nm. The instrumental performance is demonstrated by the PR spectroscopy of the well-studied bulk GaAs and GaN from UV to near-infrared spectral region. This VUV-PR system is technically operable and efficient for practical use to probe critical-point energies of the electronic band structures in semiconductors.

2. System configuration

We first briefly remind the basic principle of PR spectroscopy. Normally, a pumping beam excites the sample to generate electron–hole pairs and modify the built-in electric field. Subsequently, the material's reflection coefficient is perturbed and its reflectance intensity experiences subtle deviation at the energy corresponding to direct interband transitions. Experimentally, a probing beam illuminates the sample and its reflectance R off the sample surface as a function of photon energy is monitored. A modulated pumping laser beam focuses on the sample at the same point and causes a subtle deviation ΔR in R. Because PR spectroscopy in the form of $\Delta R/R$ is on the order of 10^{-6}–10^{-4}, a phase-sensitive lock-in amplifier (LIA) is also used to synchronously extract ΔR from the prominent reflectance signal R and background noise.

To construct a PR system based on VUV laser, one must design high vacuum chamber and optimize the corresponding optical system with optical beam paths, UV-enhanced mirror coatings, diffraction gratings, and VUV-enhanced detector. Also, it is practically sophisticated to adjust the collimation of the VUV laser and probing beam and align optical elements, as the VUV beam is strongly absorbed by the ambient air and all optics have to be placed in vacuum or chamber filled with inert gas. The detailed configuration is depicted in Fig. 1. The system is composed of three modularized parts: (i) Pumping module with the VUV laser, (ii) high vacuum chamber with cryostat, and (iii) probing and acquisition module. The design principles and techniques are introduced in the following.

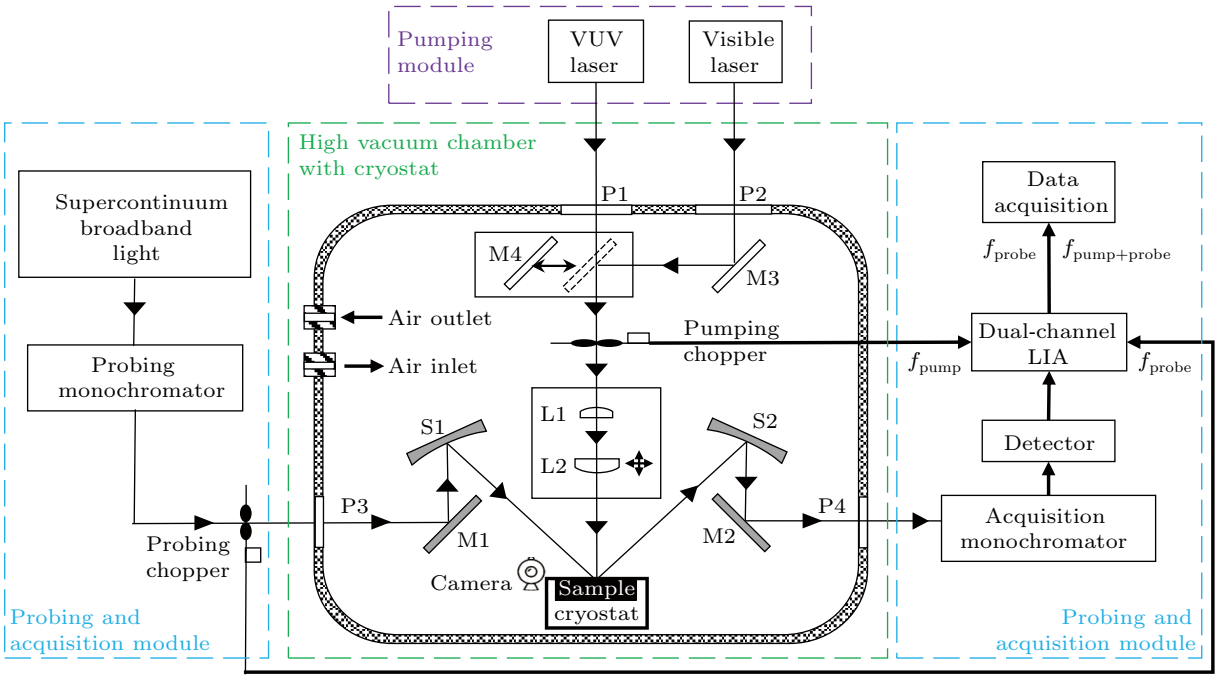


Fig. 1. Configuration of the PR system based on a VUV laser at 177.3 nm.

2.1. Pumping module with VUV laser

The VUV laser used in this system is DUV-DPL with emission at 177.3 nm, which is achieved from the second harmonic generation from a picosecond 355-nm laser using the KBBF crystal. Due to the strong absorption of 177-nm photons in air, all optics, including the KBBF crystals, are placed in a chamber filled with high-purity nitrogen. The VUV laser has pulse duration of 12 ps and repetition rate of 120 MHz. The average output power exceeds 1 mW as an effective pump-

ing beam in PR spectroscopy measurement. More details of the DUV-DPL mechanism can be found in Refs. [11,12,19]. Since VUV beam is strongly absorbed in the atmosphere and all the optics are placed in chamber, this VUV laser is also designed to include a visible laser at 633 nm for sake of pre-alignment of the optical elements and couple into this system. The pumping module also includes another alternative visible laser, which is exposed in the ambient air and can be quickly switched for any other lasers. As discussed in the introduction, the use of pumping beams with different wavelengths in beneficial for separating PR signals from the surface and complex inner structure due to their different penetration depths. This can extend the functionality of this PR system for probing distribution in multilayered films and superlattices in practical applications.

2.2. High vacuum chamber with cryostat

All the optics in the light path are placed in a vacuum chamber to avoid the strong absorption of the atmospheric environment. The vacuum chamber can maintain a high vacuum degree of 1.9×10^{-6} hPa. The chamber has an air outlet connecting to a molecular pump for vacuum evacuation and an air inlet for vacuum release. All optical components are optimized for VUV region to enhance the transmission efficiency of the VUV laser. The MgF_2 optical windows with wide transparency range are equipped on the VUV laser entrance port (P1), alternative laser entrance port (P2), probing light port (P3), and acquisition port (P4). In the beam path inside the high vacuum chamber, plane mirror (M1) and spherical mirror (S1) are used to align the probing beam from P3 and focus onto the sample surface, while plane mirror (M2) and spherical mirror (S2) are used to efficiently collect the reflected light from the sample surface and collimate into P4, as demonstrated in Fig. 1. The mirror orientation can be finely adjusted by picomotors under the vacuum condition. This optical design can guarantee high collection efficiency for reflectance signals and suppression of Rayleigh line and background noise. The mirrors are all Al-MgF_2 coated which have a low extinction coefficient to enhance reflectivity down into the VUV spectral region. Additionally, UV light irradiation is effective for oxygen desorption from the sample surface, which is reported to reduce surface Fermi level and surface electric field in PR measurement. Consequently, the PR amplitude decreases largely when the ambient medium of the sample is changed from air to vacuum.[20] A vacuum environment can help to reveal the intrinsic modulation of the pumping beam and avoid misinterpretation of PR spectra. In order to guarantee that the probed area can be fully modulated by the pumping laser, the laser spot was designed to overlap the illuminated probing spot. The laser spot of VUV laser has millimeter-size on the sample surface. The size of the probed spot on the sample can be adjustable by the slit of the excitation monochromator. In order to reduce the amount of Rayleigh line signals being collected along with reflectance signals, the pumping laser is designed to focus onto the sample at near normal incidence to maximize the absorption in the sample. A reflecting mirror (M3) and mechanically movable mirror (M4) are used for switching the 177.3 nm to the alternative 532-nm laser. The lens L1 and L2 are optimized for collimation on the sample. L1 and L2 are made of CaF_2. L2 is mounted on an x–y–z manipulated motor to coordinate with L1 for the position adjustment and collimation at the two laser wavelengths under vacuum. Since it is difficult to check the sample position and coincidence situation under vacuum, a camera is equipped to capture live images of the sample surface.

A closed-cycle cryostat refrigerator system (CCS-XG-HV/204N, Janis Research Company, Inc.) composed of Helium compressor, cold head, and cryostat is integrated in the chamber. Helium exchange gas transfers heat and cools the sample in the process. The cold head is suspended within an exchange gas chamber of nitrogen. The sample is mounted on the cold finger extension allowing temperature varying between 8 K to 325 K. The cryostat is equipped with a vibration isolation system to reduce vibration from the operation of the cold head, as well as a vertical translation system allowing adjusting the height of the sample holder under vacuum. The thermometer is provided on the sample mount of the cold finger extension for monitoring and varying the sample temperature.

2.3. Probing and acquisition module with dual-channel LIA for synchronic demodulation

Since the reflectance variation due to modulation of the pumping laser is normally more than four orders of magnitude smaller than the reflectance itself, the stability of the probing light is quite crucial during the measurement to avoid signal deviation. Continuous emission in the VUV region is also necessary for high energy probing. Xenon arc lamps was usually used to provide as probing source in UV to visible region and quartz tungsten halogen lamp in visible and near-infrared region. Instead of those, a laser-driven light source (EQ-99, Energetiq Technology Inc.) with ultra-high brightness and long-term power stability is integrated in the VUV-PR system. This light source exhibits broad-band light from 170 nm through visible and beyond, which assures the system's capability for shorter wavelength extension.

Photoreflectance system use a double monochromators configuration to synchronously scan during the measurement.[21] The excitation monochromator provide monochromatic probing beam by dispersing the supercontinuum light source, while emission monochromator acts as a tunable narrow bandpass filter to suppress spurious signals

such as luminescence and Rayleigh scattering to improve the signal-to-noise ratio. Therefore, no filters are required in front of the monochromators or detector. The two monochromators (HORIBA, iHR550) with 550-mm focal length are equipped with 300 gr/mm, 1200 gr/mm, and 1800 gr/mm gratings. All the optics in the monochromators are also MgF_2-coated. The monochromator can be insulated with nitrogen gas for the purpose to work in the VUV range. A single-channel solid state silicon detector is equipped in the emission monochromator for signal acquisition.

PR signals are normally measured by LIA with the pumping modulation frequency as the reference due to the phase-sensitive technique. Only the signals carrying the modulation frequency can be isolated from signals with other frequency components. But spurious signals such as photoluminescence (PL) from the sample, which also carries modulation frequency of the pumping laser, can be also collected. The PL signal coincides with and even swamps the PR features around the bandgap energy, particularly for the measurement on semiconductors with a direct bandgap or at low temperatures, which are disadvantageous for PR measurement.[22] To overcome aforementioned situation, dual-modulated technique was utilized to filter off PL signal and improve signal-to-noise ratio, in which both the pumping and probing beams are modulated by the corresponding choppers at different frequencies.[23,24] The PR intensity is defined as $\Delta R/R = (R_0 - R)/R_0$, where R and R_0 are the reflectance intensity with and without pumping. The reflectance intensity under dual-modulation technique has the amplitude modulation form of

$$\begin{aligned} R &= [R_0 + \Delta R \sin(2\pi f_{\text{pump}} t)] \sin(2\pi f_{\text{probe}} t + \phi) \\ &= R_0 \sin(2\pi f_{\text{probe}} t + \phi) \\ &\quad + \frac{\Delta R}{2} \cos\left[2\pi (f_{\text{probe}} - f_{\text{pump}}) t + \phi\right] \\ &\quad - \frac{\Delta R}{2} \cos\left[2\pi (f_{\text{probe}} + f_{\text{pump}}) t + \phi\right]. \end{aligned}$$

Then, R_0 can be obtained uniquely from the component with frequency of f_{probe}. ΔR can be obtained either from the component with sum frequency $f_{\text{probe}} + f_{\text{pump}}$ or difference frequency $f_{\text{probe}} - f_{\text{pump}}$. Then PR signal can be spectrally separated from PL and any other laser-related signals. This VUV-PR system uses this dual-modulated configuration with the pumping chopper housed at laser path and probing chopper at the export of excitation monochromator.

Since a slight change in the pumping or probing intensities could lead to serious variation in reflectance intensity, separate acquisition and demodulation of ΔR and R_0 is not desired from the experimental view. Early attempt of synchronic demodulation of ΔR and R_0 was accomplished by tandem demodulation by using two separate LIAs at respective reference frequency[25] or tandem LIA with digital signal processor.[26] However, to recover the amplitude of ΔR, a third LIA is necessary to demodulate the phase ϕ. The different integral time constant, gain, and phase stability between LIAs may result in more signal errors and lower accuracy. Here we use a digital dual-channel LIA (HF2LI, Zurish Instruments) contains 2 input channels, which can simultaneously demodulate at the three frequencies f_{probe} and $f_{\text{probe}} \pm f_{\text{pump}}$. This dual-channel LIA ensures the correct phase relationship for the demodulations and eliminates redundant analog-to-digital (AD) and digital-to-analog (DA) conversions. In this PR system, the frequency of pump chopper and probe chopper are fed into the LIA together. It has more than two demodulators to simultaneously extract f_{probe} and $f_{\text{probe}} + f_{\text{pump}}$ components, which facilitates quick calibration and avoids short-term fluctuations caused by unstable pumping or probing light.

The multiple choppers and dual-channel LIA also facilitate the VUV-PR system for the multifunctional realization in a single setup. It should be noted that, although dual-modulated configuration can enhance the detecting sensitivity of the fine structures in the interband transitions around bandgap energy by getting rid of the interference of PL signals, the signal intensity is reduced by a factor of $1/\pi$ than that in single-modulated configuration.[27] As an option, this VUV-PR system can switch for single-modulated PR measurement when only the pumping chopper is activated and the reflectance signal carrying the frequency of f_{probe} is demodulated. Alternatively, the system can further switch for PL measurement when only the pumping chopper is activated and the PL signal carrying the frequency of f_{pump} is demodulated.

3. System performance

To validate the system's performance, we measured and compare the PR spectroscopy of well-studied GaAs and GaN. The pumping laser beam was chopped at $f_{\text{pump}} = 177$ Hz, and the chopping frequency of probing light f_{probe} is set at 220 Hz. Both $f_{\text{probe}} - f_{\text{pump}}$ and $f_{\text{probe}} + f_{\text{pump}}$ carry the ΔR signal. In order to avoid the interference of the frequency multiplication of $f_{\text{probe}} - f_{\text{pump}}$, the sum frequency $f_{\text{probe}} + f_{\text{pump}}$ is preferred for demodulation of ΔR.[28] The standard fitting procedure with a model[29] of the third derivative functional form $\Delta R/R = \text{Re}[\sum_{j=1}^{m} C_j e^{i\theta_j}(E - E_j + i\Gamma_j)^{-n}]$ is applied, where C_j and θ_j are the resonance amplitude and phase angle of the line shape, E is the photon energy, E_j and Γ_j are the energy and the broadening parameter of the j-th transition, respectively. The exponent n depends on the type of critical point in the Brillouin zone.

As shown in Fig. 2, $n = 2.5$ was used for fitting of semi-insulating GaAs.[30] No signs of Franz–Kyldysh oscillations appear in PR spectra indicating that the modulation is within the low electric field region. The derived critical points are marked by vertical arrows. The spectral features near the

bandgap at $E_0 = 1.43$ eV and $E_0 + \Delta_0 = 1.76$ eV are well-resolved, which correspond to the fundamental transition and the transition between the conduction band and spin–orbit splitting valence subband at Γ point of the Brillouin zone, respectively. The origin of the interband transition marked with asterisk is not determined but it also appears under 532-nm pumping,[3] further studies are required to clarify this. The spectral features above the bandgap at $E_1 = 2.94$ eV and $E_1 + \Delta_1 = 3.18$ eV correspond to the transition along the Λ direction in Brillouin zone. These features are in good accordance with previous reports by PR and ER spectroscopy.[1] In the UV region, according to the interband energies of GaAs derived from the dielectric function,[31] the spectral features can be attributed to interband transitions at the Γ point of Brillouin zone: $E_0'(\Gamma_8^v - \Gamma_7^c) = 4.45$ eV, $E_0' + \Delta_0'(\Gamma_8^v - \Gamma_8^c) = 4.69$ eV, and $E_0' + \Delta_0' + \Delta_0(\Gamma_7^v - \Gamma_8^c) = 5.04$ eV. A higher feature at $E_2(X) = 5.46$ eV is assigned to the transition at X point of Brillouin zone, which is not clearly resolved under 532-nm pumping.[3] The experimental results agree well with calculated critical points energies[32] and results derived by spectroscopic ellipsometry.[31] The spectral feature related to $E_0' + \Delta_0'$ has an amplitude of 2×10^{-5}, which demonstrates a sensitivity better than 10^{-5} level can be warranted by this system.

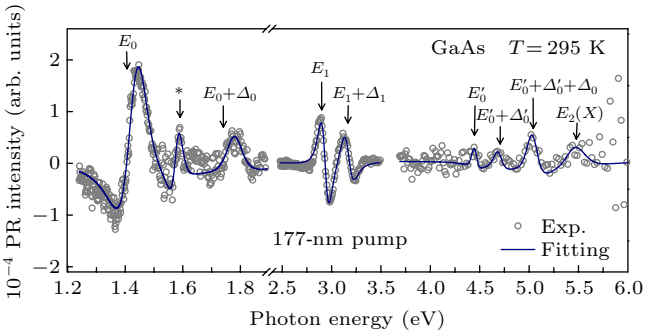


Fig. 2. Dual-modulated PR spectra of semi-insulating GaAs pumped at 177.3 nm. The gray circles show the experimental data and solid lines the fitting results. The arrows indicate the corresponding interband transitions.

The photoreflectance system based on VUV laser at 177.3 nm was also applied to investigate PR spectra of wurtzite GaN on Al_2O_3 at 8 K and 295 K, as shown in Fig. 3. GaN is a typical well-studied wide bandgap semiconductor and has prominent PL signal under UV excitation, which can be avoided in this dual-modulated configuration. $n = 2$ is used to fit the PR spectra in accordance with previous reports.[33] The energy positions obtained by fitting are indicated by the vertical arrows in Fig. 3. The well-resolved features are related to excitonic transitions corresponding to previous report:[6,33] A: exciton ($\Gamma_9^v - \Gamma_7^c$), B: exciton (Γ_7^v(upper band) $- \Gamma_7^c$), and C: exciton (Γ_7^v(lower band) $- \Gamma_7^c$). The exciton energy can be slightly dependent on crystal growth condition, different residual biaxial compressive strains, film thicknesses, and electron concentrations in GaN/sapphire epitaxial layers.[34,35] At 8 K, the energy positions of the A, B, and C excitons are fitted to be 3.457 eV, 3.465 eV, and 3.476 eV, respectively. The energy separation of A and B excitons of 8 meV agrees well with that in reported PR measurement.[36] As the temperature increases, the PR spectral features would gradually broaden and shift towards lower energy. At 295 K, the energy positions of the A, B, and C excitons are derived at 3.388 eV, 3.401 eV, and 3.422 eV, respectively. The splitting among A, B, and C excitonic transition energies become slightly larger and C exciton becomes quite weak as the temperature increases, which is also similar to previous reports.[6,33] The above results demonstrate this VUV-PR system can be used to determine the interband transition energies of GaN with high spectral resolution.

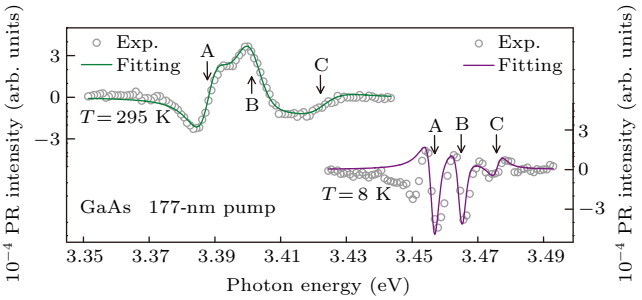


Fig. 3. Dual-modulated PR spectra of wurtzite GaN pumped at 177.3 nm at 8 K and 295 K, respectively. The gray circles show the experimental data and solid lines the fitting results. The arrows indicate the corresponding excitonic transition energies.

4. Conclusion

Modularized dual-modulated VUV-PR system was designed and constructed, which is composed of three modularized parts: (i) pumping module with a VUV laser, (ii) high vacuum chamber, and (iii) probing and acquisition module. We demonstrate the capability of VUV laser at 177.3 nm can be serviced as an efficient pumping laser beam to measure PR spectroscopy, which allows for the investigation of the electronic band structure of semiconductors in the DUV to near-infrared spectral range.

Acknowledgments

Project supported by the National Development Project for Major Scientific Research Facility of China (Grant No. ZDYZ2012-2), the National Natural Science Foundation of China (Grant No. 11874350), and CAS Key Research Program of Frontier Sciences (Grant Nos. ZDBS-LY-SLH004 and XDPB22).

References

[1] Glembocki O J and Shanabrook B V 1992 *Semiconductors and Semimetals (Elsevier)* **36** pp. 221–292
[2] Kudrawiec R and Misiewicz J 2012 *Semiconductor Research: Experimental Techniques* (Berlin, Heidelberg: Springer) pp. 95–124
[3] Liu X L, Wu J B, Luo X D and Tan P H 2017 *Acta Phys. Sin.* **66** 147801 (in Chinese)
[4] Fuertes Marrón D 2017 *Int. J. Photoenergy* **2017** 4894127

[5] Bhimnathwala H and Borrego J M 1992 *Solid State Electron.* **35** 1503
[6] Kudrawiec R, Rudziński M, Serafinczuk J, Zając M and Misiewicz J 2009 *J. Appl. Phys.* **105** 093541
[7] Sotnikov A E, Chernikov M A, Ryabushkin O A, Trubenko P, Moshegov N and Ovchinnikov A 2004 *Quantum Electron.* **34** 871
[8] Zhang R, Yang K, Qin L H, Shen B, Shi H T, Shi Y, Gu S L, Zheng Y D, Huang Z C and Chen J C 1996 *J. Vac. Sci. Technol. A* **14** 840
[9] Bru-Chevallier C, Fanget S, Guillot G, Ruffenach S and Briot O 2004 *Thin Solid Films* **450** 75
[10] Munguía J, Chouaib H, de la Torre J, Bremond G, Bru-Chevallier C, Sibai A, Champagnon B, Moreau M and Bluet J M 2006 *Nucl. Instrum. Methods Phys. Res. B* **253** 18
[11] Chen C T, Xu Z Y, Deng D Q, Zhang J, Wong G K L, Wu B C, Ye N and Tang D 1996 *Appl. Phys. Lett.* **68** 2930
[12] Togashi T, Kanai T, Sekikawa T, Watanabe S, Chen C T, Zhang C Q, Xu Z Y and Wang J Y 2003 *Opt. Lett.* **28** 254
[13] Lin Z Q, Chen W B, Lou Q H, Fan W, Xiang S Q and Xue H B 2013 *Sci. China Technol. Sci.* **56** 1571
[14] Jin S Q, Fan F T, Guo M L, Zhang Y, Feng Z C and Li C 2014 *Rev. Sci. Instrum.* **85** 046105
[15] Zhang H Y, Wu H M, Jia Y H, Geng L J, Luo Z X, Fu H B and Yao J N 2019 *Rev. Sci. Instrum.* **90** 073101
[16] Ning Y X, Fu Q, Li Y F, Zhao S Q, Wang C, Breitschaft M, Hagen S, Schaff O and Bao X H 2019 *Ultramicroscopy* **200** 105
[17] Wang Z H, Pan S H, Huang S, Zhang C Z and Mu S M, Zhou X C, Jian J, Xu G C and Chen Z K 1993 *J. Phys. D: Appl. Phys.* **26** 1493
[18] Shi L, Nihtianov S, Haspeslagh L, Scholze F, Gottwald A and Nanver L K 2012 *IEEE Trans. Electron Dev.* **59** 2888
[19] Peng Q J, Zong N, Zhang S J, Wang Z M, Yang F, Zhang F F, Xu Z Y and Zhou X J 2018 *IEEE J. Sel. Top Quantum Electron.* **24** 1
[20] Behn U, Thamm A, Brandt O and Grahn H T 2000 *J. Appl. Phys.* **87** 4315
[21] Theis W M, Sanders G D, Leak C E, Bajaj K K and Morkoc H 1988 *Phys. Rev. B* **37** 3042
[22] Zhang B and Wang X J 2017 *Rev. Sci. Instrum.* **88** 106103
[23] Lu C R, Anderson J R, Stone D R, Beard W T and Wilson R A 1990 *Superlattices Microstruct.* **8** 155
[24] Ghosh S and Arora B M 1995 *IEEE J. Sel. Top Quantum Electron.* **1** 1108
[25] Amirtharaj P M, Chandler-Horowitz D and Bour D P 1995 *MRS Online Proceedings Library* **406** 229
[26] Qin J H, Huang Z M, Ge Y J, Hou Y and Chu J H 2009 *Rev. Sci. Instrum.* **80** 033112
[27] Ghosh S and Arora B M 1998 *Rev. Sci. Instrum.* **69** 1261
[28] Ho C H, Hsieh C H, Chen Y J, Huang Y S and Tiong K K 2001 *Rev. Sci. Instrum.* **72** 4218
[29] Aspnes D E 1973 *Surf. Sci.* **37** 418
[30] Wang R Z and Jiang D S 1992 *J. Appl. Phys.* **72** 3826
[31] Lautenschlager P, Garriga M, Logothetidis S and Cardona M 1987 *Phys. Rev. B* **35** 9174
[32] James R C and Marvin L C 1974 *Phys. Rev. Lett.* **32** 674
[33] Li C F, Huang Y S, Malikova L and Pollak F H 1997 *Phys. Rev. B* **55** 9251
[34] Viswanath A K, Lee J I, Yu S, Kim D, Choi Y and Hong C 1998 *J. Appl. Phys.* **84** 3848
[35] Kudrawiec R, Sęk G, Misiewicz J, Paszkiewicz R, Paszkiewicz B and Tłaczała M 2002 *Mater. Sci. Eng. B* **96** 284
[36] Shan W, Little B D, Fischer A J, Song J J, Goldenberg B, Perry W G, Bremser M D and Davis R F 1996 *Phys. Rev. B* **54** 16369